Autophagy promotes cell survival by maintaining NAD(H) levels

Lucia Sedlackova
Newcastle University
Tetsushi Kataura
Newcastle University
Elena Seranova
University of Birmingham
Congxin Sun
University of Birmingham
Elsje Otten
MRC Laboratory of Molecular Biology https://orcid.org/0000-0002-8716-3560
Malkiel Cohen
Whitehead Institute for Biomedical Research
Miruna Chipara
University of Birmingham
Adina Palhegyi
University of Birmingham
David Shapira
Newcastle University
Filippo Scialo
Newcastle University
Rhoda Stefanatos
Newcastle University
Kei-ichi Ishikawa
Juntendo University
Niall Kenneth
University of Liverpool
Tong Zhang
University of Glasgow
Prashanta Panda
University of Birmingham
Malgorzata Zatyka
University of Birmingham
Luiz Silva

University of Birmingham
Jorge Torresi
University of Birmingham
Kevin Kauffman
David H. Koch Institute for Integrative Cancer Research, Massachusetts Institute of Technology
Shupei Zhang
Whitehead Institute for Biomedical Research
Dorothea Maetzel
Whitehead Institute for Biomedical Research
Thiago Varga
University of Birmingham
Carl Ward
Guangzhou Institutes of Biomedicine and Health, Chinese Academy of Sciences
https://orcid.org/0000-0003-0889-9025
David Cartwright
University of Birmingham
Gareth Lavery
University of Birmingham
Gaurav Sahay
Oregon State University
Yosef Buganim
The Hebrew University-Hadassah Medical School
Daniel Anderson
Massachusetts Institute of Technology https://orcid.org/0000-0001-5629-4798
Animesh Acharjee
University of Birmingham https://orcid.org/0000-0003-2735-7010
Charles Bascom
The Procter and Gamble Company
Ryan Tasseff
The Procter and Gamble Company
Robert Isfort
The Procter and Gamble Company
John Oblong
The Procter and Gamble Company
Joerg Gsponer
University of British Columbia
Satomi Miwa
Newcastle University
Michael Lazarou

Monash University https://orcid.org/0000-0003-2150-5545
Manolis Papamichos-Chronakis
University of Liverpool
Haoyi Wang
State Key Laboratory of Reproductive Biology
Masaya Imoto
Keio University
Shinji Saiki
Juntendo University School of Medicine
Oliver Maddocks
University of Glasgow https://orcid.org/0000-0002-5551-9091
Alberto Sanz
University of Glasgow
Tatiana Rosenstock
University of Birmingham
Rudolf Jaenisch
Massachusetts Institute of Technology https://orcid.org/0000-0002-2540-7099
Viktor Korolchuk
Newcastle University https://orcid.org/0000-0002-4071-592X
Sovan Sarkar (S.Sarkar@bham.ac.uk)
University of Birmingham https://orcid.org/0000-0002-9456-4362

Article

Keywords: autophagy, cell survival, nicotinamide adenine dinucleotide (NAD+/NADH)

Posted Date: July 12th, 2021

DOI: https://doi.org/10.21203/rs.3.rs-659023/v1

Abstract

Autophagy is an essential catabolic process that promotes the clearance of surplus or damaged intracellular components[1]. As a recycling process, autophagy is also important for the maintenance of cellular metabolites to aid metabolic homeostasis[2]. Loss of autophagy in animal models or malfunction of this process in a number of age-related human pathologies, including neurodegenerative and lysosomal storage diseases, contributes to tissue degeneration[3-9]. However, it remains unclear which of the many cellular functions of autophagy primarily underlies its role in cell survival. Here we have identified an evolutionarily conserved role of autophagy from yeast to humans in the preservation of nicotinamide adenine dinucleotide (NAD+/NADH) levels, which are critical for cellular survival. In respiring cells, loss of autophagy caused hyperactivation of PARP and Sirtuin families of NADases. Uncontrolled depletion of NAD(H) pool by these enzymes resulted in mitochondrial membrane depolarisation and cell death. Supplementation with NAD(H) precursors improved cell viability in autophagy-deficient models including human pluripotent stem cell-derived neurons with autophagy deficiency or patient-derived neurons with autophagy dysfunction. Our study provides a mechanistic link between autophagy and NAD(H) metabolism, and suggests that boosting NAD(H) levels may have therapeutic benefits in human diseases associated with autophagy dysfunction.

Main

Autophagy is a cellular trafficking pathway mediated by the formation of double-membraned vesicles called autophagosomes, which ultimately fuse with lysosomes where their cargo is degraded. By sequestering and clearing dysfunctional cellular components, such as protein aggregates and damaged organelles, autophagy maintains cellular homeostasis whilst also providing metabolites and energy during periods of starvation[2]. Studies using a range of laboratory models from yeast to mammals have established that autophagy is essential for cellular and organismal survival. For example, loss of an essential autophagy gene *atg5* leads to reduced survival of *Saccharomyces cerevisiae* in nitrogen starvation conditions and shortened lifespan in *Drosophila melanogaster*[10,11]. Likewise, inducible knockout of *Atg5* results in cell death and neurodegeneration in adult mice[3,12,13]. It remains unclear which of the many physiological functions of autophagy are most important for its role in maintaining cell and organismal survival. Furthermore, the role of autophagy in the quality control of cellular proteins and organelles is likely to impact a plethora of signal transduction and stress response pathways, which in turn affect metabolism, growth, and survival[14,15]. Untangling this complexity *in vivo* is challenging whilst mechanistic studies of the cellular roles of autophagy *in vitro* are hindered by the fact that autophagy-deficient cells are viable in cell culture[12,13,16]. We hypothesized that this apparent discrepancy between the requirement for functional autophagy *in vivo* and *in vitro* could be due to a metabolic shift from oxidative phosphorylation (OXPHOS) to glycolysis in tissue culture, which could mask an underlying viability defect in autophagy-deficient cells[17].

Cell death underlying loss of autophagy was associated with NAD(H) depletion

A well-established strategy to reverse cellular reliance on energy generation via aerobic glycolysis and promote mitochondrial OXPHOS is to replace glucose, the major carbon source in tissue culture media, with galactose[18-22]. Strikingly, *Atg5*$^{-/-}$ but not wild-type mouse embryonic fibroblasts (MEFs) cultured in galactose media displayed rapid (~24 h) caspase activation and cell death (Fig. 1a, b, Extended Data Fig. 1a). This phenotype was not caused by galactose directly as it was not toxic in the presence of glucose (Extended Data Fig. 1b, c). Instead, it was driven by mitochondrial respiration since its suppression by hypoxia or mitochondrial pyruvate carrier inhibitor UK-5099 was sufficient to rescue cell death (Extended Data Fig. 1d-g). Specificity of this phenotype was validated by re-expression of Atg5, and the apoptotic nature of cell death as evidenced by caspase 3 cleavage was confirmed using Z-VAD-fmk (Extended Data Fig. 2a-c). A similar phenotype was observed in cell lines with CRISPR/Cas9 knockout of key autophagy genes such as *Atg5*, *Atg7* or *Rb1cc1* (homologue of human *FIP200*), as well as with the loss of lysosomal cholesterol transporter Npc1 required for efficient autophagy[6] (Fig. 1c, Extended Data Fig. 2d, e).

The rapid nature of cell death suggested an underlying metabolic collapse in autophagy-deficient cells[23]. Loss of autophagy was previously shown to cause depletion of cellular metabolites, although the mechanisms linking these metabolic defects to the cell death phenotype are poorly understood[2]. To investigate the potential metabolic basis of cell death due to autophagy deficiency, we performed an unbiased metabolomics profiling of wild-type and *Atg5*$^{-/-}$ MEFs after 16 h in galactose media, i.e., prior to the onset of cell death. In agreement with a previously proposed general defect in nucleic acid recycling in autophagy-deficient cells[24], a number of nucleotides were depleted in *Atg5*$^{-/-}$ MEFs (Fig. 1d, Extended Data Fig. 3a-c). By plotting the magnitude of change against the measure of significance, we identified the reduced form of nicotinamide adenine dinucleotide (NADH) as the most significantly depleted metabolite in autophagy-deficient cells (Fig. 1d, Extended Data Fig. 3b). NAD^+, the oxidized form of the NAD dinucleotide, was also significantly decreased, suggesting that autophagy-deficient cells present with a depletion of the total pool of the NAD(H) (Fig. 1d, Extended Data Fig. 3b, c). We further confirmed NAD(H) deficit via a fluorescence-based assay in *Atg5*$^{-/-}$ MEFs (Fig. 1e).

Evolutionarily conserved role of autophagy in maintaining NAD(H) levels

Autophagy is required for the survival of eukaryotic organisms from yeast to man[25]. We investigated whether the role of autophagy in the maintenance of intracellular NAD(H) pools is evolutionarily conserved. Knockdown of *Atg5* in the fruit fly, *Drosophila melanogaster*, reduced autophagic flux as was evident from accumulation of autophagy substrate Ref(2)P[26], and resulted in significant depletion of NAD(H) (Fig. 1f, Extended Data Fig. 3d). We further analyzed nitrogen-deprived *Saccharomyces cerevisiae* yeast that are dependent on mitochondrial respiration, wherein autophagy deficiency causes loss of respiratory capacity and cell death[11]. We found that nitrogen-deprived *atg5Δ* yeast exhibited both the loss of autophagy flux as monitored by Atg8-GFP cleavage[26] and a striking depletion of NAD(H) levels (Fig. 1g, Extended Data Fig. 3e). Together with our observations in MEFs, these data imply an evolutionary-conserved role of autophagy in the preservation of NAD(H) levels.

Increased NADase activity mediated NAD(H) depletion in autophagy-deficient cells

We further investigated the role of NAD(H) in mediating cytotoxicity underlying autophagy deficiency. Inhibition of nicotinamide phosphoribosyltransferase (NAMPT) involved in NAD biosynthesis via a salvage pathway[27] (Fig. 2a) by FK866 compromised the viability of wild-type MEFs in galactose, but not glucose, medium, indicating that NAD(H) is a limiting factor for the survival of OXPHOS-dependent cells (Extended Data Fig. 4a, b). We therefore investigated the mechanism of NAD(H) depletion in autophagy-deficient cells. Activities of two main classes of NAD-consuming enzymes, poly-ADP-ribose polymerases (PARPs) and deacetylases of sirtuin family (SIRTs)[28], were increased in *Atg5*$^{-/-}$ MEFs after 14 h culture in galactose media. This was evident from elevated levels of poly-ADP-ribosylation (PARylation) and reduced protein acetylation, respectively (Fig. 2b). PARylation, but not deacetylation, activity remained elevated after 20 h of culture (Extended Data Fig. 4c), consistent with the reliance of SIRTs but not PARPs on high cellular NAD^+ levels[15]. SIRTs and PARPs are activated by reactive oxygen species (ROS) and DNA damage that were found to be significantly elevated in respiring *Atg5*$^{-/-}$ MEFs (Extended Data Fig. 4d-h), likely resulting from mitochondrial dysfunction due to loss of autophagic quality control[14,29]. Indeed, OXPHOS-dependent *Atg5*$^{-/-}$ MEFs displayed disrupted mitochondrial morphology, altered levels of electron transport chain supercomplexes, and reduced ATP generation via OXPHOS (and increased reliance on glycolysis in glucose media) (Extended Data Fig. 4i-l).

We did not find evidence for PARP hyperactivation as a direct cause of cell death which is mediated by the mitochondria-to-nucleus translocation of apoptosis-inducing factor (AIF) (Extended Data Fig. 5a). Therefore, we hypothesized that the loss of cell viability is triggered by NAD(H) exhaustion due to uncontrolled NAD^+ cleavage. Indeed, pharmacological inhibition of SIRTs with sirtinol or PARPs with olaparib partially rescued both, intracellular NAD(H) levels and cell viability of *Atg5*$^{-/-}$ MEFs (Fig. 2a, c, d, Extended Data Fig. 5b-d). The role of NADases was further validated by siRNA-mediated knockdown of *Sirt1* or *Parp1*, indicating involvement of these enzymes in NAD(H) depletion and cell death (Extended Data Fig. 5e-h).

Boosting intracellular NAD(H) rescued viability of autophagy-deficient cells

To test whether boosting intracellular NAD(H) levels is sufficient to rescue viability of autophagy-deficient cells, we utilized the native cellular capacity for NAD^+ synthesis (Fig. 2a). Supplementation of bioavailable NAD^+ precursors, nicotinamide (NAM) or nicotinamide riboside (NR), led to the recovery of intracellular NAD^+ and NADH levels, and rescued viability of *Atg5*$^{-/-}$ MEFs (Fig. 2e, f, Extended Data Fig. 6a). The effect of NAM (but not NR) was abrogated by FK866 (Fig. 2e, f, Extended Data Fig. 6a), consistent with the requirement for conversion of these precursors to NAD(H) via the salvage pathway (Fig. 2a). Both precursors also inhibited PARP and/or SIRT activity[28] (Extended Data Fig. 6b). However, rescue of NAD(H) and cell viability did not correlate with PARPs/SIRTs activity because FK866, which also suppressed PARylation/deacetylation by reducing NAD(H) levels, did not rescue cell viability (Fig. 2e, f, Extended Data Fig. 6a, b). Furthermore, in the presence of FK866, NR (but not NAM which requires

NAMPT for conversion to NAD^+) improved NAD(H) levels and cell viability whilst PARylation/deacetylation activity was instead partially rescued compared to FK866 alone (Fig. 2e, f, Extended Data Fig. 6a, b). We conclude that boosting NAD(H) levels rescued cell death downstream of PARPs/SIRTs.

We performed an unbiased metabolomics profiling of *Atg5*$^{-/-}$ MEF in galactose medium, treated with or without NAM, to assess any correlation between the rescue of cell death and recovery of intracellular metabolites. By plotting the magnitude of rescue against the measure of significance, we found NADH to be the only metabolite that primarily correlated with *Atg5*$^{-/-}$ MEF viability, i.e., it was first found to be significantly depleted in *Atg5*$^{-/-}$ MEF (Fig. 1d, Extended Data Fig. 3b, c) and then significantly restored by NAM supplementation (Fig. 2g, Extended Data Fig. 6c, d). NAD^+ followed a similar trend (Fig. 1d, 2g, Extended Data Fig. 3b, c, 6c, d). Therefore, the rescue of cell death is mediated by increased NAD(H), but not, for example, ATP (Fig. 2g, Extended Data Fig. 6c, d). The role of NAD(H), but not PARP/SIRT directly, was further supported by NAD(H) supplementation via *de novo* pathway using L-tryptophan (Fig. 2a), which rescued NAD(H) levels and cell death whilst having no inhibitory effect on PARP/SIRT activities (Fig. 2h, i, Extended Data Fig. 6e, f). Together, the salvage and *de novo* pathways remain active in autophagy-deficient cells and NAD(H) depletion is primarily mediated by its increased consumption.

Since *Atg5*$^{-/-}$ MEFs manifested with general nucleotide depletion (Fig. 1d, Extended Data Fig. 3b, c), we supplemented cells in galactose medium with five nucleosides and found that all were able to restore cell viability whilst NAD(H) levels were not rescued (Extended Data Fig. 7a-c). Therefore, NAD(H) decline is independent of the previously proposed purine/pyrimidine depletion mechanism of cell death in autophagy-deficient tumor-derived cells[24]. Inhibition of Nrf2, previously shown to mediate cell death in autophagy deficiency[30], also rescued viability without affecting NAD(H) levels (Extended Data Fig. 7d-f). Therefore, NAD(H) decline is an additional and previously unidentified cause of cell death due to autophagy deficiency.

NAD(H) depletion mediated cell death via mitochondrial depolarization

NADH was predominantly detected in a mitochondria-enriched cell fraction where it was depleted in *Atg5*$^{-/-}$ MEFs cultured in galactose medium (Fig. 3a). Oxidation of NADH generates mitochondrial membrane potential ($\Delta\Psi m$) across the inner mitochondrial membrane and we hypothesized that depletion of mitochondrial NADH is the cause of mitochondrial depolarization and apoptosis[14,31]. Indeed, boosting NAD(H) levels with NAM rescued membrane depolarization in *Atg5*$^{-/-}$ MEFs (Fig. 3b, c). Furthermore, preventing dissipation of $\Delta\Psi m$ by suppressing ATP synthase activity (using a low dose of oligomycin)[32], partially prevented depletion of NADH and rescued cell death (Fig. 3b-e, Extended Data Fig. 8a). Consistent with no effect of oligomycin on NAD^+ levels (Fig. 3d), SIRT and PARP activities remained unaffected (Extended Data Fig. 8b), indicating that oligomycin acted downstream. To further test the role of mitochondrial NADH in the cell death phenotype, we overexpressed a non-proton pumping alternative NADH oxidase, NDI1[33]. In galactose medium, overexpression of NDI1 led to an increased oxidation state

of the NAD(H) pool which was sufficient to enhance the apoptotic phenotype of *Atg5*$^{-/-}$ MEFs (Fig. 3f, g, Extended Data Fig. 8c, d). We conclude that NADH is the limiting factor in the survival of autophagy-deficient cells.

Generation of autophagy-deficient human neurons from *ATG5*$^{-/-}$ hESCs

To test the relevance of our findings in a physiologically relevant human system, we employed autophagy-deficient (*ATG5*$^{-/-}$) human neurons by harnessing the pluripotency property of human embryonic stem cells (hESCs). Towards this, we first generated *ATG5*$^{-/-}$ hESCs by knockout of *ATG5* exon 3 via genome editing with transcription activator-like effector nucleases (TALENs) (Extended Data Fig. 2d, 9a, b). *ATG5*$^{-/-}$ hESCs expressed pluripotency markers, such as NANOG, SOX2, OCT4, SSEA4 and TRA-1-60, comparable to wild-type (*ATG5*$^{+/+}$) hESCs (Extended Data Fig. 9c-e). Loss of autophagy was confirmed by the absence of ATG5-ATG12 conjugate and LC3-II (autophagosomes), and accumulation of p62 (autophagy substrate)[26] in *ATG5*$^{-/-}$ hESCs (Extended Data Fig. 10a-d). Multiple clones of *ATG5*$^{-/-}$ hESCs were differentiated into neural precursors (NPs) and then to neurons, which were confirmed for their cellular identity with cell-specific markers (Fig. 4a, Extended Data Fig. 11a-e) and loss of autophagy (Fig. 4b, c, Extended Data Fig. 11f-h). Further validation of our hESC-based human cellular platforms with autophagy deficiency was made by complementing *ATG5*$^{-/-}$ hESCs with human *ATG5* mRNA via lipid nanoparticles (LNPs), formulated with the ionizable lipid C12-200[34] (Extended Data Fig. 12a). C12-200 LNP-mediated delivery of human *ATG5* mRNA, but not *GFP* mRNA, generated the ATG5-ATG12 conjugate and restored functional autophagic flux in *ATG5*$^{-/-}$ hESCs and neurons (Extended Data Fig. 12b-e).

Loss of NAD(H) underlies cytotoxicity in human neurons with autophagy deficiency

We next investigated the mechanistic link between NAD(H) and cell survival in human neurons. While hESCs rely on glycolysis for energy production and pluripotency[35], differentiated cells like neurons with high energy demands are dependent on mitochondrial OXPHOS for ATP generation[36]. This allows analysis in neurons to be performed at basal state by eliminating the need for medium switch to galactose. We found that NAD(H) levels were significantly depleted in *ATG5*$^{-/-}$ hESC-derived neurons 3 weeks after differentiation (Fig. 4d), further supporting the evolutionarily conserved role of autophagy in maintaining NAD(H) pool (Fig. 1e-g). Since oxidation of NADH generates $\Delta\Psi m$ [14], depletion of NADH was associated with mitochondrial depolarization (Extended Data Fig. 13a). Autophagy-deficient neurons also exhibited elevation in ROS (Fig. 4e), mitochondrial fragmentation and increased mitochondrial load (Extended Data Fig. 13b-f), presumably due to accumulation of damaged mitochondria arising from abrogation of autophagic clearance. In agreement with a role of NAD-consuming enzymes in depleting NAD(H) levels, PARylation and deacetylation activities of PARPs and SIRTs, respectively, were increased in *ATG5*$^{-/-}$ hESC-derived neurons (Fig. 4f). Notably, increased cell death was observed at a basal level in *ATG5*$^{-/-}$ neurons between 2 and 4 weeks after differentiation (Fig. 4g-i, Extended Data Fig. 13g, h). Collectively, these data in autophagy-deficient human neurons were consistent with our finding in *Atg5*$^{-/-}$ MEFs.

Pharmacological elevation of NAD(H) is cytoprotective in human neurons with autophagy deficiency or dysfunction

Next, we evaluated the effects of pharmacologically modulating NAD(H) levels (Fig. 2a) on cell viability of *ATG5*$^{-/-}$ neurons. NAM increased NAD(H) levels, and consequently restored ΔΨm in *ATG5*$^{-/-}$ hESC-derived neurons (Fig. 5a, b). These changes were associated with improvement in axonal length and rescue of cell death in *ATG5*$^{-/-}$ neurons after NAM treatment, which did not affect ATP or ADP levels (Fig. 5c-f, Extended Data Fig. 14a-c). NR also rescued the viability of *ATG5*$^{-/-}$ neurons (Extended Data Fig. 14d, e). Inhibition of NAD(H) production by FK866 further augmented cell death in *ATG5*$^{-/-}$ neurons (Extended Data Fig. 15a-d) and abolished the cytoprotective effect of NAM (Fig. 5f), thus implying a role of NAD(H) in governing neuronal survival.

Finally, we utilized disease-affected human neurons differentiated from patient-derived human induced pluripotent stem cells (hiPSCs) of a neurodegenerative lysosomal storage disorder, Niemann-Pick type C1 (NPC1) disease. As previously reported[37], NPC1 neurons presented with a severe autophagic defect (Extended Data Fig. 16a-c) and cell death between 3 and 4 weeks after differentiation (Fig. 5g). Similar to our findings in autophagy-deficient models, autophagy dysfunction in NPC1 neurons correlated with NAD(H) depletion (Fig. 5h). Treatment with NAM was able to rescue both, NAD(H) levels and cell death phenotype in NPC1 neurons (Fig. 5g, h), thus showing therapeutic benefits.

Discussion

We found that autophagy deficiency in respiring cells results in cell death. Whilst an accumulation of dysfunctional mitochondria contributes to increased cellular stress, the cell death is caused indirectly by the hyperactivity of stress responsive NAD^+-dependent enzymes such as SIRTs and PARPs, which ultimately lead to the loss of NAD(H) homeostasis. Exhaustion of NADH within mitochondria appears to be the weakest link in this chain of events as it ultimately triggers mitochondrial membrane depolarization and activation of apoptosis (Fig. 5i). This model where the demise of autophagy deficient cells is mediated by stress response pathways is conceptually analogous to the previously proposed mechanism involving hyperactivation of Nrf2[30]. How this and other mechanisms, such as depletion of the general nucleotide pool in autophagy-deficient cells[24], integrate with the critical role of NAD(H) depletion during autophagy deficiency remains to be investigated (Fig. 5i).

Ageing and age-related diseases have long been associated with a decline in both autophagy and NAD^+ levels[38]. Nutritional or pharmacological activation of autophagy is currently a subject of intense research for the development of small molecule modulators[7]. However, due to the varied nature of autophagy dysfunction in genetic and age-related sporadic diseases, including impairment in lysosomal degradative capability, the development of a universal modulator remains unlikely[7-9]. In contrast, boosting the levels of NAD^+ by precursor supplementation in animal models was found to have a positive impact on age-related phenotypes, which is at least in part mediated by upregulation of autophagy[38]. Crucially, our data

show that autophagy is, in turn, required for NAD(H) maintenance and that increasing NAD(H) levels protects cells by preventing the loss of ΔΨm even in the absence of functional autophagy. As such, our investigations define a novel mechanism linking autophagy, NAD(H) metabolism and ageing. Finally, our studies establish several points of intervention that could be targeted therapeutically in order to alleviate cellular pathology in a range of diseases associated with autophagy dysfunction.

Declarations

Acknowledgements: We are grateful to B. Carroll, Y. Rabanal-Ruiz, G. Kelly, F. Urselli, E. Bennet, A. Kaur, L.A. Oakey, R. Banerjee, D. Astuti, S. Vats, M. Dawlaty, K. Wert, Q. Gao, R. Alagappan, A. Huerta-Uribe, T. Barrett and J. Frampton for technical assistance or providing general reagents; N. Watson for electron microscopy; G. Nelson, W. Salmon and R. Shaw for imaging assistance; H. Salmonowicz for graphical design; M. Coleman and S. Chakrabortee for manuscript feedback; University of Birmingham IBR Technology Hub, Newcastle Bioimaging Unit and Whitehead Institute Keck Microscopy Facility. A.S. is a Senior Wellcome Fellow. So.S. and V.I.K. are also Former Fellows (life) of Hughes Hall, University of Cambridge, UK.

Funding:

This study was supported by grants from Wellcome Trust (109626/Z/15/Z, 1516ISSFFEL10), LifeArc (P2019-0004), UKIERI (2016-17-0087) and Birmingham Fellowship to So.S.; BBSRC (BB/M023389/1) and MRC studentship (BH174490) to V.I.K.; BBSRC (BB/R008167/2) to A.S. and V.I.K.; NIH (R37HD045022, R01-NS088538, R01-MH104610) to R.J.; Rutherford Fellowship, University of Birmingham (UoB) Brazil Visiting Fellowship and FAPESP-UoB to So.S. and T.R.R.; FAPESP (2015/02041-1) to T.R.R.; CRUK Fellowship (C53309/A19702) to O.D.K.M.; JSPS (18KK0242) to Sh.S., K.I., M.I. and V.I.K.; JSPS Fellowship (19J12969) to T.K.; NHMRC (GNT1106471, GNT1160315) and Australian Research Council (FT1601100063, DP200100347) to M.L.; NIHR Surgical Reconstruction and Microbiology Research Centre in Birmingham (A.A.); Emerald Foundation, LEO Foundation (L18015) and St. Baldrick's Foundation to R.J. and M.A.C.

Author Contributions:

L.S., T.K., E.S., C.S., E.G.O., M.A.C., M.C., A.M.P., D.S., F.S., R.S., K.I., N.K., T.Z., P.K.P., M.Z., L.F.S.E.S., J.T., K.J.K., S.Z., D.M., T.G.V., C.W., D.C., G.G.L., G.S., Y.B., D.G.A., A.A., J.G., S.M., H.W., O.D.K.M., T.R.R., V.I.K. and So.S. performed experiments, provided methodology or analysed data; T.K., M.A.C., K.I., L.F.S.E.S., A.A., M.L., M.I., Sh.S., O.D.K.M., A.S., T.R.R., R.J., V.I.K. and So.S. acquired funding; V.I.K. and So.S. conceptualized and administered the project, and wrote the manuscript.

Competing interests: C.C.B., R.T., R.J.I. and J.E.O. are employees of The Procter & Gamble Company, USA. R.J. is cofounder of Fate Therapeutics, Fulcrum Therapeutics and Omega Therapeutics, and advisor to Dewpoint Therapeutics. E.S. is founder of NMN Bio. All other authors declare they have no competing interests.

Ethics statement: There are no ethical requirements for the use of human embryonic stem cells (hESCs) and human induced pluripotent stem cells (hiPSCs) in this study because the parental hESC (WIBR3 hESC) and the hiPSC (control and NPC1 patient-derived hiPSCs) lines have been previously published and have undergone many passages in cell culture. The parental WIBR3 hESC and the control and NPC1 patient derived hiPSCs were originally generated in the lab of Rudolf Jaenisch at the Whitehead Institute for Biomedical Research. These cell lines were used for this study in the lab of Sovan Sarkar at the University of Birmingham under material transfer agreements, UBMTA 15-0593 and UBMTA 15-0594. All experiments were performed in accordance with ISSCR and institutional guidelines and regulations.

Materials and correspondence: Correspondence and requests for materials should be addressed to viktor.korolchuk@newcastle.ac.uk (V.I.K.) and s.sarkar@bham.ac.uk (So.S.).

Supplementary Information

Supplementary Information is available for this paper including Methods, Supplementary References 1–28, Supplementary Tables 1–5 and Extended Data Fig. 1–16.

References

1 Anding, A. L. & Baehrecke, E. H. Cleaning house: selective autophagy of organelles. *Dev. Cell* **41**, 10-22 (2017).

2 Lahiri, V., Hawkins, W. D. & Klionsky, D. J. Watch what you (self-) eat: autophagic mechanisms that modulate metabolism. *Cell Metab.* **29**, 803-826 (2019).

3 Hara, T. *et al.* Suppression of basal autophagy in neural cells causes neurodegenerative disease in mice. *Nature* **441**, 885 (2006).

4 Komatsu, M. *et al.* Loss of autophagy in the central nervous system causes neurodegeneration in mice. *Nature* **441**, 880 (2006).

5 Nakai, A. *et al.* The role of autophagy in cardiomyocytes in the basal state and in response to hemodynamic stress. *Nat. Med.* **13**, 619-624 (2007).

6 Sarkar, S. *et al.* Impaired autophagy in the lipid-storage disorder Niemann-Pick type C1 disease. *Cell Rep.* **5**, 1302-1315 (2013).

7 Menzies, F. M. *et al.* Autophagy and neurodegeneration: pathogenic mechanisms and therapeutic opportunities. *Neuron* **93**, 1015-1034 (2017).

8 Seranova, E. *et al.* Human induced pluripotent stem cell models of neurodegenerative disorders for studying the biomedical implications of autophagy. *J. Mol. Biol.* **432**, 2754-2798 (2020).

9 Seranova, E. *et al.* Dysregulation of autophagy as a common mechanism in lysosomal storage diseases. *Essays Biochem.* **61**, 733-749 (2017).

10 Bjedov, I. *et al.* Mechanisms of life span extension by rapamycin in the fruit fly Drosophila melanogaster. *Cell Metab.* **11**, 35-46 (2010).

11 Suzuki, S. W., Onodera, J. & Ohsumi, Y. Starvation induced cell death in autophagy-defective yeast mutants is caused by mitochondria dysfunction. *PloS One* **6**, e17412 (2011).

12 Cassidy, L. D. *et al.* A novel Atg5-shRNA mouse model enables temporal control of Autophagy in vivo. *Autophagy* **14**, 1256-1266 (2018).

13 Kuma, A. *et al.* The role of autophagy during the early neonatal starvation period. *Nature* **432**, 1032 (2004).

14 Sedlackova, L. & Korolchuk, V. I. Mitochondrial quality control as a key determinant of cell survival. *Biochim. Biophys. Acta Mol. Cell Res.* **1866**, 575-587 (2018).

15 Sedlackova, L. & Korolchuk, V. I. The crosstalk of NAD, ROS and autophagy in cellular health and ageing. *Biogerontology* **21**, 381-397 (2020).

16 Bampton, E. T., Goemans, C. G., Niranjan, D., Mizushima, N. & Tolkovsky, A. M. The dynamics of autophagy visualised in live cells: from autophagosome formation to fusion with endo/lysosomes. *Autophagy* **1**, 23-36 (2005).

17 To, T. L. *et al.* A compendium of genetic modifiers of mitochondrial dysfunction reveals intra-organelle buffering. *Cell* **179**, 1222-1238.e1217 (2019).

18 Robinson, B., Petrova-Benedict, R., Buncic, J. & Wallace, D. Nonviability of cells with oxidative defects in galactose medium: a screening test for affected patient fibroblasts. *Biochem. Med. Metab. Biol.* **48**, 122-126 (1992).

19 Rossignol, R. *et al.* Energy substrate modulates mitochondrial structure and oxidative capacity in cancer cells. *Cancer Res.* **64**, 985-993 (2004).

20 Marroquin, L. D., Hynes, J., Dykens, J. A., Jamieson, J. D. & Will, Y. Circumventing the Crabtree effect: replacing media glucose with galactose increases susceptibility of HepG2 cells to mitochondrial toxicants. *Toxicol. Sci.* **97**, 539-547 (2007).

21 Iannetti, E. F., Smeitink, J. A., Willems, P. H., Beyrath, J. & Koopman, W. J. Rescue from galactose-induced death of leigh syndrome patient cells by pyruvate and NAD+. *Cell Death Dis.* **9**, 1135 (2018).

22 Stroud, D. A. *et al.* Accessory subunits are integral for assembly and function of human mitochondrial complex I. *Nature* **538**, 123 (2016).

23 Altman, B. J. & Rathmell, J. C. Metabolic stress in autophagy and cell death pathways. *Cold Spring Harb. Perspect. Biol.* **4**, a008763 (2012).

24 Guo, J. Y. *et al.* Autophagy provides metabolic substrates to maintain energy charge and nucleotide pools in Ras-driven lung cancer cells. *Genes Dev.* **30**, 1704-1717 (2016).

25 Levine, B. & Kroemer, G. Biological functions of autophagy genes: a disease perspective. *Cell* **176**, 11-42 (2019).

26 Klionsky, D. J. *et al.* Guidelines for the use and interpretation of assays for monitoring autophagy (4th edition)(1). *Autophagy* **17**, 1-382 (2021).

27 Hasmann, M. & Schemainda, I. FK866, a highly specific noncompetitive inhibitor of nicotinamide phosphoribosyltransferase, represents a novel mechanism for induction of tumor cell apoptosis. *Cancer Res.* **63**, 7436-7442 (2003).

28 Cantó, C., Sauve, A. A. & Bai, P. Crosstalk between poly(ADP-ribose) polymerase and sirtuin enzymes. *Mol. Aspects Med.* **34**, 1168-1201 (2013).

29 Hewitt, G. & Korolchuk, V. I. Repair, reuse, recycle: the expanding role of autophagy in genome maintenance. *Trends Cell Biol.* **27**, 340-351 (2017).

30 Komatsu, M. *et al.* The selective autophagy substrate p62 activates the stress responsive transcription factor Nrf2 through inactivation of Keap1. *Nat. Cell Biol.* **12**, 213-223 (2010).

31 Abramov, A. Y. & Duchen, M. R. Mechanisms underlying the loss of mitochondrial membrane potential in glutamate excitotoxicity. *Biochim. Biophys. Acta* **1777**, 953-964 (2008).

32 Perry, S. W., Norman, J. P., Barbieri, J., Brown, E. B. & Gelbard, H. A. Mitochondrial membrane potential probes and the proton gradient: a practical usage guide. *Biotechniques* **50**, 98-115 (2011).

33 Scialò, F. *et al.* Mitochondrial ROS Produced via Reverse Electron Transport Extend Animal Lifespan. *Cell Metab.* **23**, 725-734 (2016).

34 Kauffman, K. J. *et al.* Optimization of lipid nanoparticle formulations for mRNA delivery in vivo with fractional factorial and definitive screening designs. *Nano Lett.* **15**, 7300-7306 (2015).

35 Gu, W. *et al.* Glycolytic metabolism plays a functional role in regulating human pluripotent stem cell state. *Cell Stem Cell* **19**, 476-490 (2016).

36 Zheng, X. *et al.* Metabolic reprogramming during neuronal differentiation from aerobic glycolysis to neuronal oxidative phosphorylation. *Elife* **5**, e13374 (2016).

37 Maetzel, D. *et al.* Genetic and chemical correction of cholesterol accumulation and impaired autophagy in hepatic and neural cells derived from Niemann-Pick Type C patient-specific iPS cells. *Stem*

Cell Rep. **2**, 866-880 (2014).

38 Hansen, M., Rubinsztein, D. C. & Walker, D. W. Autophagy as a promoter of longevity: insights from model organisms. *Nat. Rev. Mol. Cell Biol.* **19**, 579-593 (2018).

Figures

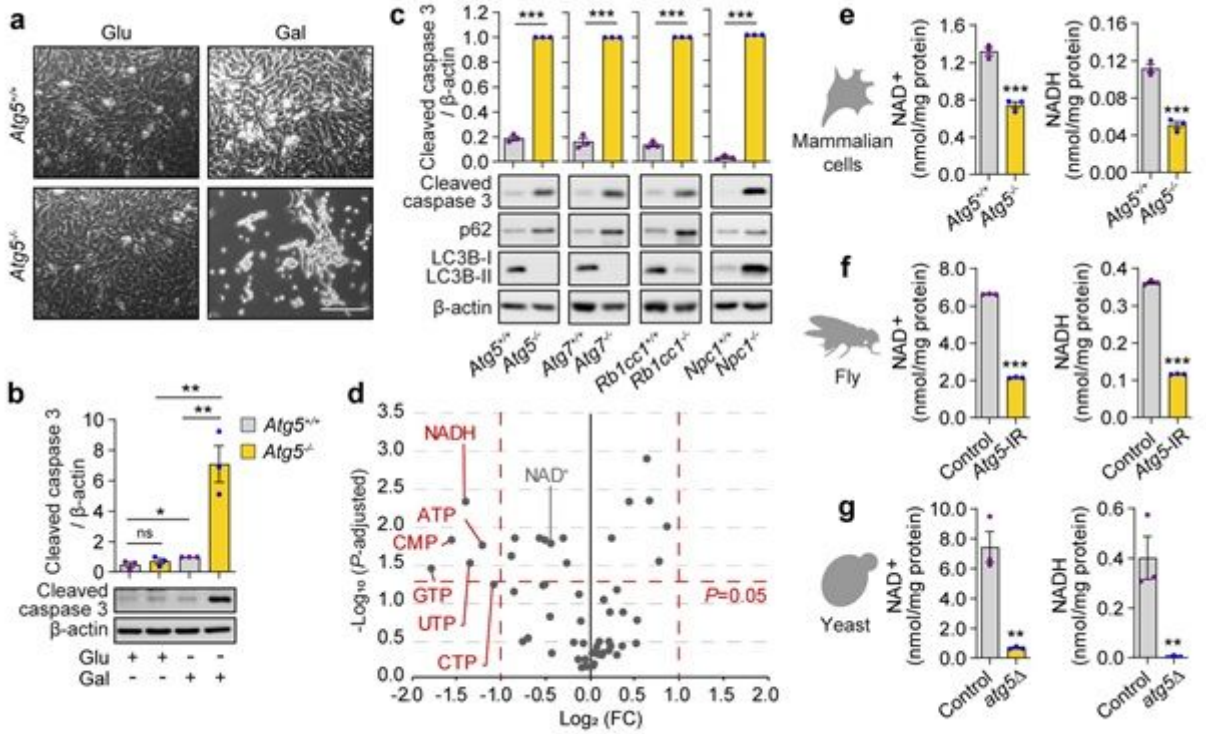

Figure 1

Metabolic deficit in respiring autophagy-incompetent cells and animal models. a, b, Phase contrast images (a) and immunoblot analyses (b) of Atg5+/+ or Atg5-/- MEFs cultured in glucose (glu) or galactose (gal) medium for 24 h. c, Immunoblotting analyses of isogenic Atg5+/+ and Atg5-/-, Atg7+/+ and Atg7-/-, Rb1cc1+/+ and Rbcc1-/- cell lines generated by the CRISPR-Cas9 system; and Npc1+/+ and Npc1-/- MEFs grown in gal medium for 110 h (Atg5, Atg7 and Rb1cc1 CRISPR-Cas9 generated cell lines) and 72 h (Npc1 cell lines). d, Volcano plot representation of all analyzed metabolites in a pairwise comparison of Atg5-/- to Atg5+/+ MEFs after 16 h in gal medium. Thresholds are shown as dashed red lines. e–g, NAD+ and NADH measurements of Atg5+/+ or Atg5-/- MEFs cultured in glu or gal medium for 16 h (e), control (daGAL4>ATTP2) and ATG5-IR (daGAL4>ATG5-IR) 20-day-old flies fed on standard media at 25 oC (20 flies per group) (f), and control and atg5Δ yeast strains following 3 days of nitrogen starvation (g). Graphical data are mean ± s.e.m. of n = 3 biological replicates (b, c, e–g). P values were calculated by unpaired two-tailed Student's t-test (b, c, e–g) or the multiple t-test original FDR method of Benjamini and Hochberg (d) on three independent experiments. *P<0.05; **P<0.01; ***P<0.001; ns (non-significant). Scale bar, 200 μm (a).

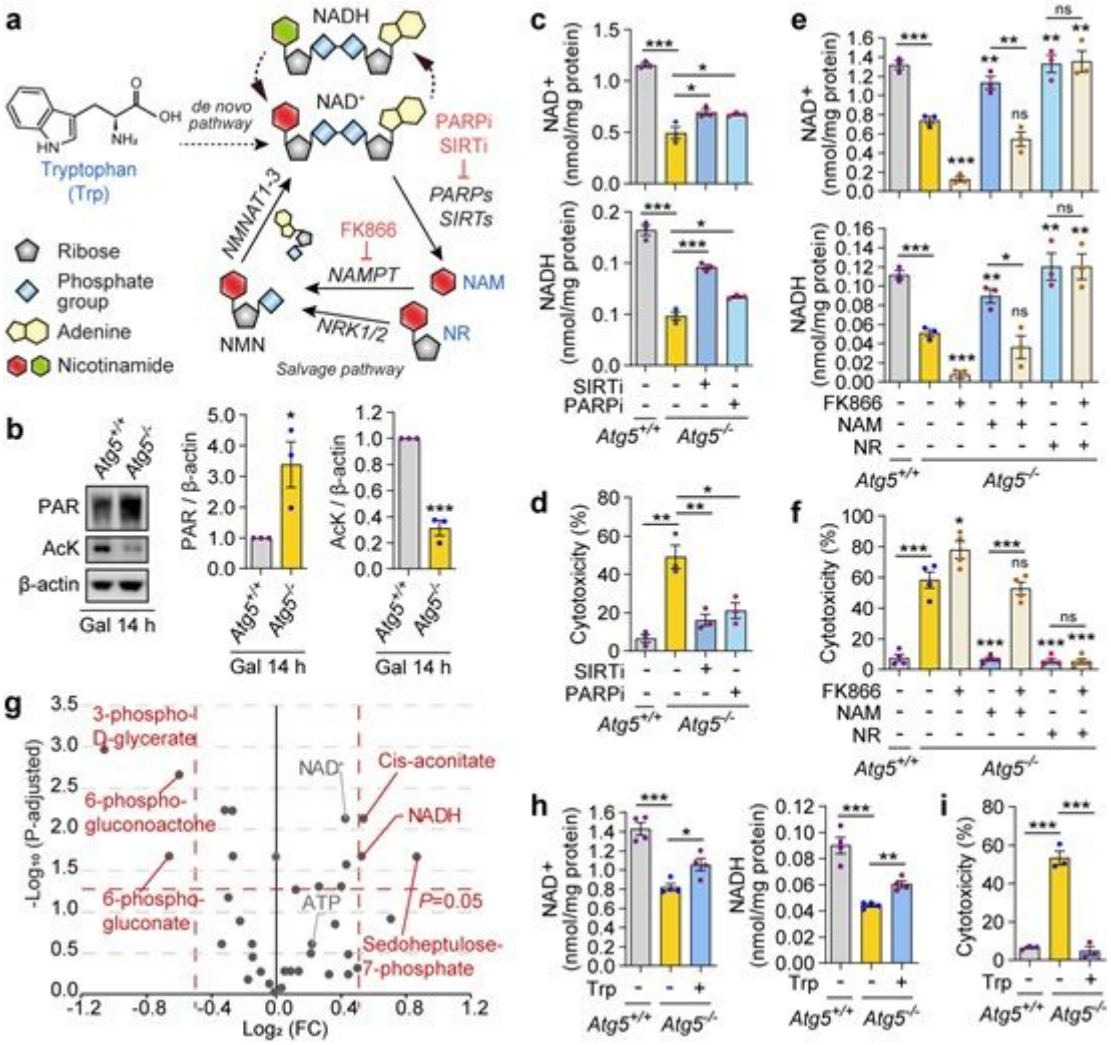

Figure 2

NAD(H) depletion contributes to cell death due to autophagy deficiency. a, Graphical representation of the NAD+ synthesis pathways. Enzyme inhibitors are highlighted in red. b, Immunoblot analyses for acetylated lysine (AcK) and poly(ADP-ribose) (PAR) in Atg5+/+ and Atg5-/- MEFs cultured in galactose (gal) medium for 14 h. c–f, Measurement of NAD+ and NADH (c, e) and cytotoxicity assays (d, f) in Atg5+/+ and Atg5-/- MEFs cultured for 20 h (c, e) or 40 h (d, f) in gal medium supplemented with sirtinol (SIRTi), olaparib (PARPi) or solvent (DMSO) (c, d), or with NAM or NR in the presence or absence of FK866 (e, f). g, Volcano plot representation of all analyzed metabolites in a pairwise comparison of Atg5-/-+NAM to Atg5-/- MEFs cultured in gal medium for 16 h. Thresholds are shown as dashed red lines. h, i, Measurement of NAD+ and NADH and cytotoxicity assays in Atg5+/+ and Atg5-/- MEFs cultured for 20 h (h) or 40 h (i) in gal medium supplemented with L-tryptophan (Trp). Graphical data are mean ± s.e.m. of n = 3–4 biological replicates as indicated (b–f, h, i). P values were calculated by unpaired two-tailed Student's t-test (b–f, h, i) or the multiple t-test original FDR method of Benjamini and Hochberg (g) on three independent experiments. *P<0.05; **P<0.01; ***P<0.001; ns (non-significant).

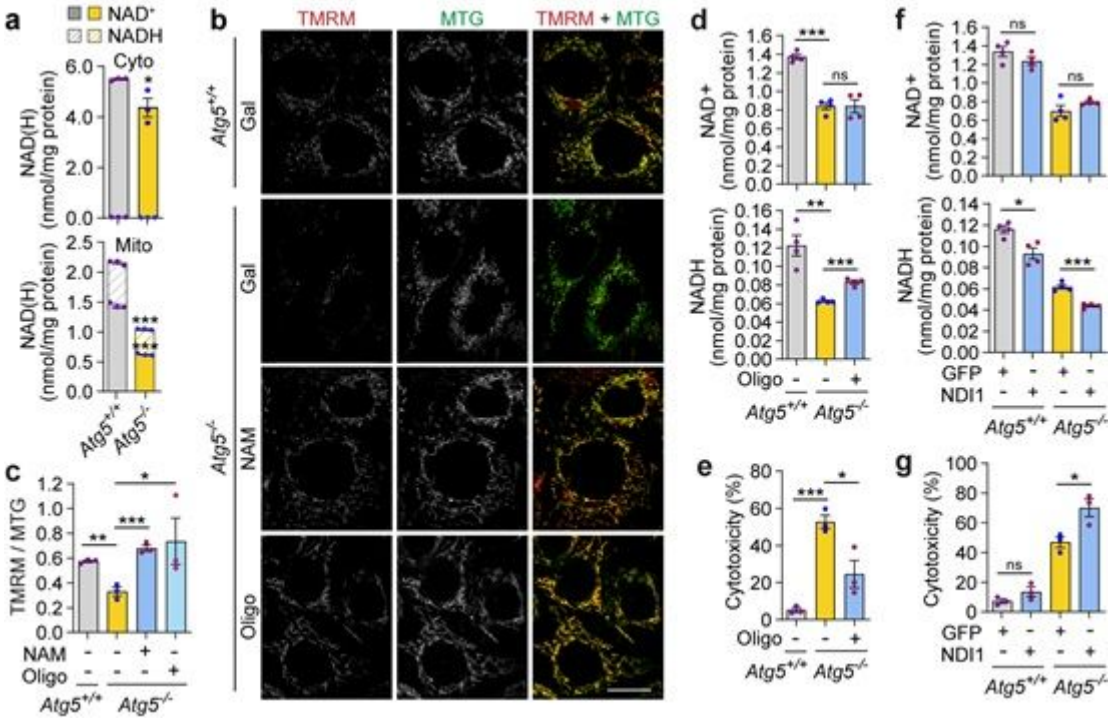

Figure 3

Depletion of mitochondrial NADH underlies loss of autophagy-deficient cell viability. a, Measurement of NAD+ and NADH levels in cytoplasmic (cyto) and mitochondrial (mito) fractions of Atg5+/+ and Atg5-/- MEFs after 20 h culture in galactose (gal) medium. b, Confocal immunofluorescence images of live cells after 20 h culture in gal medium supplemented with NAM or oligomycin (Oligo) and co-stained with TMRM and MTG. c, ΔΨm quantified as a ratio of TMRM to MTG. d–g, Measurement of NAD+ and NADH levels (d, f) or cytotoxicity assays (e, g) in Atg5+/+ and Atg5-/- MEFs treated with Oligo or solvent (DMSO), or in Atg5+/+ and Atg5-/- MEFs transfected with GFP-NDI1 (NDI1) or an empty plasmid (GFP), after 20 h (d, f) or 40 h (e, g) culture in gal medium. Graphical data are mean ± s.e.m. of n = 3–4 biological replicates as indicated (a, c, d–g). P values were calculated by unpaired two-tailed Student's t-test on three independent experiments (a, c, d–g). *P<0.05; **P<0.01; ***P<0.001; ns (non-significant). Scale bar, 20 μm (b).

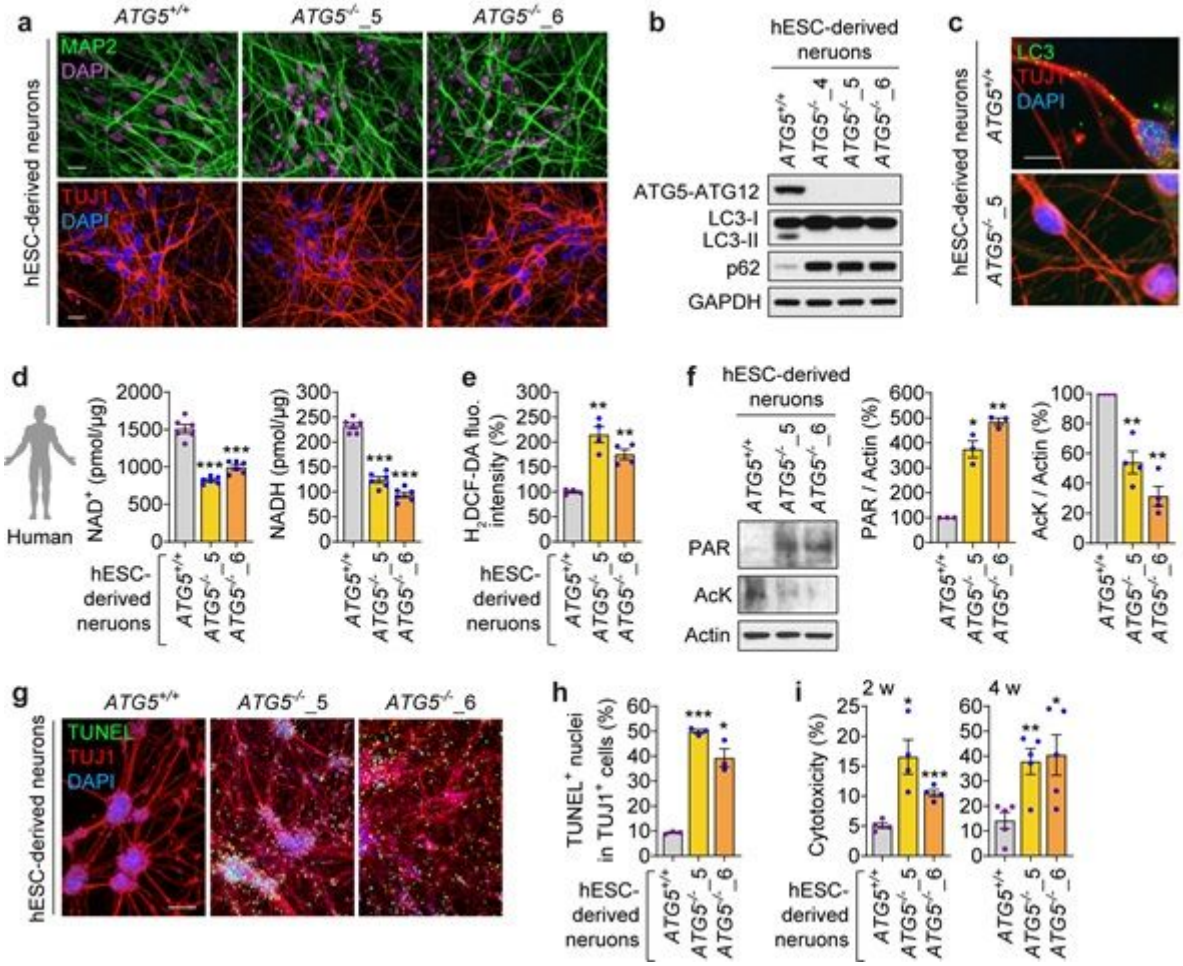

Figure 4

Autophagy-deficient human neurons manifest with NAD(H) depletion and cell death. a–c, Immunofluorescence images of MAP2 and TUJ1 (a), immunoblotting analyses of ATG5, LC3, p62 and GAPDH (b) and immunofluorescence images of LC3 and TUJ1 (c) in ATG5+/+ and multiple clones of ATG5−/− hESC-derived neurons (4-weeks). d–h, Measurements of NAD+ and NADH levels (d) and H2DCF-DA fluorescence intensity (e), immunoblotting analyses for poly(ADP-ribose) (PAR) and acetylated lysine (AcK) (f), and immunofluorescence images of TUJ1 with TUNEL staining (g) and quantification of TUNEL+ apoptotic nuclei (h) in ATG5+/+ and ATG5−/− hESC-derived neurons (3-weeks). i, Cytotoxicity assay in ATG5+/+ and ATG5−/− hESC-derived neurons at 2 or 4 weeks (w) of neuronal differentiation. Graphical data are mean ± s.e.m. of n = 3–6 biological replicates as indicated (d–f, h, i). P values were calculated by unpaired two-tailed Student's t-test on two (e, i) or three (d, f, h) independent experiments. *P<0.05; **P<0.01; ***P<0.001. Scale bar, 10 µm (c) or 100 µm (a, g).

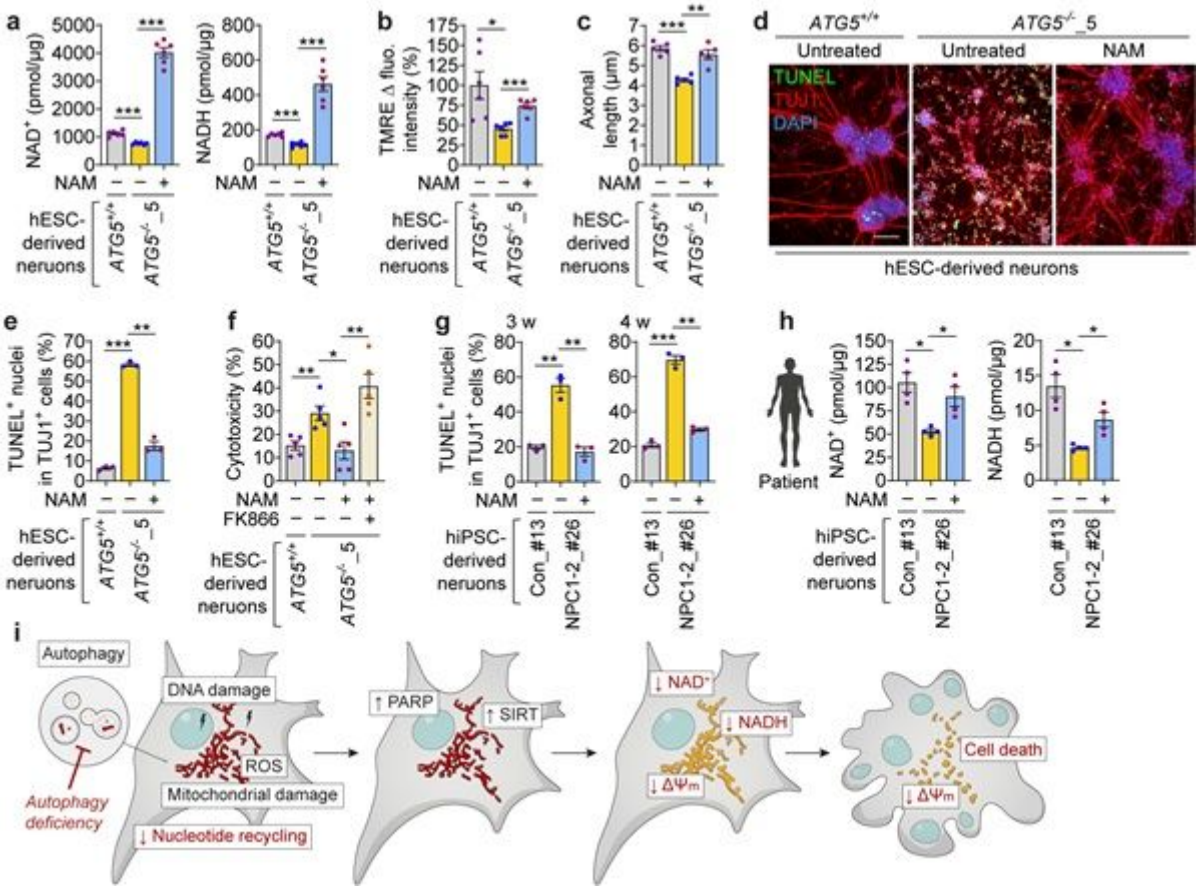

Figure 5

Boosting NAD(H) improves cell viability in human neurons with autophagy deficiency or dysfunction. a–e, Measurements of NAD+ and NADH levels (a), TMRE Δ fluorescence intensity (b) and axonal length (c), and immunofluorescence images of TUJ1 with TUNEL staining (d) and quantification of TUNEL+ apoptotic nuclei (e) in ATG5+/+ and ATG5−/− hESC-derived neurons (3-weeks), where ATG5−/− neurons were treated with or without NAM for the last 6 days. f, Cytotoxicity assay in ATG5+/+ and ATG5−/− hESC-derived neurons (3-weeks), where ATG5−/− neurons were treated with NAM in the presence or absence of FK866 for the last 6 days. g, h, Quantification of TUNEL+ apoptotic nuclei in TUJ1+ cells (g) and measurements of NAD+ and NADH levels (h) in control (Con) and NPC1 hiPSC-derived neurons after 3 (g, h) or 4 (g) weeks of neuronal differentiation, where NPC1 neurons were treated with or without NAM for the last 6 days. i, Schematic representation of the mechanism of NAD(H) depletion leading to mitochondrial depolarization and apoptosis in respiring autophagy-deficient cells. Graphical data are mean ± s.e.m. of n = 3–6 biological replicates as indicated (a–c, e–h). P values were calculated by unpaired two-tailed Student's t-test on two (b, f) or three (a, c–e, g, h) independent experiments. *P<0.05; **P<0.01; ***P<0.001. Scale bar, 100 µm (d).

Supplementary Files

This is a list of supplementary files associated with this preprint. Click to download.

- SedlackovaetalNatureCellBiologySupplementaryInformation.docx
- SedlackovaetalNCBS46014TSupplementaryInformation.docx